



Geochemical and statistical evidence of recharge, mixing, and controls on spring discharge in an eogenetic karst aquifer

Paul J. Moore^{*}, Jonathan B. Martin, Elizabeth J. Screaton

Department of Geological Sciences, 241 Williamson Hall, P.O. Box 112120, University of Florida, Gainesville, FL 32611-2120, United States

ARTICLE INFO

Article history:

Received 20 November 2008

Received in revised form 7 June 2009

Accepted 20 July 2009

This manuscript was handled by P. Bavey, Editor-in-Chief

Keywords:

Floridan aquifer

Karst springs

Chemistry

Mixing

Recharge

SUMMARY

Information about sources of recharge, distributions of flow paths, and the extent of water–rock reactions in karst aquifers commonly result from monitoring spring chemistry and discharge. To investigate the relationship between spring characteristics and the complexities of karst aquifers, we couple variations in surface- and groundwater chemistry to physical conditions including river stage, precipitation, and evapotranspiration (ET) within a sink-rise system through a 6-km portion of the Upper Floridan aquifer (UFA) in north-central Florida. Principal component analysis (PCA) of time series major-element compositions suggests that at least three sources of water affect spring discharge, including allogenic recharge into a swallet, diffuse recharge through a thin vadose zone, and water upwelling from deep within the aquifer. The deep-water source exerts the strongest influence on water chemistry by providing a majority of Na^+ , Mg^{2+} , K^+ , Cl^- , and SO_4^{2-} to the system. Anomalously high temperature at one of several monitoring wells reflects vertical flow of about 1 m/year. Mass-balance calculations suggest diffuse recharge and deep-water upwelling can provide up to 50% of the spring discharge; however, their contributions depend on head gradients between the conduit and surrounding aquifer matrix, which are influenced by variations in precipitation, ET, and river stage. Our results indicate that upwelling from deep flow paths may provide significant contributions of water to spring discharge, and that monitoring only springs limits interpretations of karst systems by masking critical components of the aquifer, such as water sources and flow paths. These results also suggest the matrix in eogenetic aquifers is a major pathway for flow even in a system dominated by conduits.

© 2009 Elsevier B.V. All rights reserved.

Introduction

Karst aquifers are characterized by heterogeneous distributions of various types of porosity including intergranular porosity within the matrix rock, fractures along joints, faults and bedding planes, and conduits enlarged through dissolution. This porosity distribution influences nearly all aspects of aquifer characteristics, including aquifer storage and distribution of permeability. The range of porosity and permeability determines flow paths and allows extreme flow rates including both laminar and turbulent flow (Worthington, 1994; Quinlan et al., 1996; White, 1999; Halihan et al., 2000). While most flow in karst aquifers occurs through conduits, storage is primarily in the matrix porosity (e.g., Worthington et al., 2000). Matrix porosity and permeability also affect recharge to the aquifer, which can vary on seasonal and individual storm time scales. Karst aquifer recharge commonly occurs as point source

(allogenic) recharge into swallets or as diffuse recharge through the vadose zone (e.g., White, 1988; Ford and Williams, 2007). Upward flow of water from deep within an aquifer may also contribute to an aquifer's shallow-water budget and chemistry, depending on the distribution of porosity, permeability, and hydraulic head (Kohout et al., 1977; Smith and Fuller, 1977; Hughes et al., 2007). Assessing origins of water, which is needed to understand susceptibility of karst areas to contamination, requires a clear understanding of processes causing variations in groundwater chemistry and connectivity between conduit and matrix porosity (e.g., McConnell and Hacke, 1993; Plummer et al., 1998; Katz, 2004).

Flow paths and sources of recharge to karst aquifers have long been assessed through physical, chemical, and isotopic variations in springs (e.g., Shuster and White, 1971; Krothe and Libra, 1983; Dreiss, 1989). These studies commonly use chemical and isotopic changes to separate sources of water from storm recharge (quick flow) and drainage from the matrix porosity (base flow) (e.g., Lakey and Krothe, 1996). In most well-studied cases, springs are in regions with dense, recrystallized rocks (i.e., telogenetic karst, Vacher and Mylroie, 2002), where low matrix permeability restricts most of the flow to conduits and fracture networks. Individual

^{*} Corresponding author. Present address: ExxonMobil Exploration Company, 233 Benmar Drive, Houston, TX 77060, United States. Tel.: +1 352 392 2231; fax: +1 352 392 9294.

E-mail addresses: pjm13@ufl.edu (P.J. Moore), jbmartin@ufl.edu (J.B. Martin), screaton@ufl.edu (E.J. Screaton).

springs exhibiting large variations in discharge and chemical composition through time have been inferred to be dominated by allogenic recharge and conduit flow. In contrast, springs with smaller amounts of chemical variability and discharge have been inferred to be dominated by diffuse recharge and diffuse flow through fracture networks (Shuster and White, 1971; Ternan, 1972; Smart and Hobbs, 1986; Hess and White, 1988; Dreiss, 1989; Lee and Krothe, 2001). These studies assume that spring variability results largely from variation in recharge and the flow paths of that recharge. Considering only these few parameters limits the understanding of the karst system that can be derived from variations in spring-water chemistry. For example, physical and chemical variations in springs issuing from the karstic Inner Bluegrass region of Kentucky fail to reflect the geometry of the aquifer's conduit system because differences in lengths of flow paths mask variations in conduit sizes that source the springs (Scanlon and Thraillkill, 1987). Consequently, a question we explore in this paper is what additional insight can be gained from physical and chemical monitoring of spring flow and chemical composition.

Large springs also discharge from carbonate rocks that retain high matrix porosity and permeability (i.e., eogenetic karst, Vacher and Mylroie, 2002). In these rocks, high matrix permeability allows access to aquifer storage and diffuse recharge, which constitute a substantial component of spring discharge (e.g., Florea and Vacher, 2006; Ritorto et al., 2009). Numerous springs that discharge from the eogenetic Upper Floridan aquifer (UFA) appear to be fed primarily from diffuse recharge transmitted through the rock matrix (e.g., Martin and Gordon, 2000; Katz, 2004; Florea and Vacher, 2006). Other springs discharging from the UFA are directly connected by conduits to allogenic inputs so that the source of water to these springs depend on the hydraulic head gradient between the conduit and surrounding aquifer matrix (Katz et al., 1998; Screaton et al., 2004; Loper et al., 2005; Martin et al., 2006). When allogenic inputs allow conduit hydraulic head to exceed head in the surrounding matrix, allogenic recharge accounts for most to all of

the spring discharge, with an additional fraction of the recharge stored temporarily in the matrix until the flood pulse recedes and hydraulic head gradients reverse (e.g., Screaton et al., 2004; Martin et al., 2006). Following head reversal, spring discharge is a mixture of water stored temporarily in the matrix, allogenic recharge, and water recharged diffusely to the matrix from the surface. This interaction between allogenic recharge and diffusely recharged water can lead to high variability in discharge and spring-water chemistry (e.g., Katz et al., 1998; Crandall et al., 1999; Katz et al., 2001; Martin and Dean, 2001; Katz et al., 2004; Screaton et al., 2004; Martin et al., 2006).

In this paper we use major-element chemistry, physical conditions including river stage, precipitation, evapotranspiration (ET), temperature gradients of groundwater, and a multivariate statistical method (principal component analysis; PCA) to evaluate how multiple sources of water and variations in aquifer flow paths influence a first-magnitude spring draining a portion of the eogenetic UFA. We suggest that knowledge of the spatial and temporal variation of groundwater chemistry is necessary to separate sources of water and components of flow, which cannot be resolved by only monitoring spring discharge, and that mixing of these water sources plays an important role in temporal variations of spring chemistry. Because of the importance of groundwater sources to spring-water chemistry, matrix porosity in eogenetic aquifers appears to be significant to spring discharge even where dominated by conduits.

Study area

The Santa Fe River is a tributary of the Suwannee River, with a watershed covering about 3600 km² in north-central Florida (Hunn and Slack, 1983). Land use in the watershed is mainly agricultural, primarily as improved pastures and row and field crops (Kautz et al., 2007). In the watershed, Oligocene and Eocene carbonate rocks make up the UFA (Fig. 1). The aquifer is confined by the Haw-

Series		Hydrostratigraphic Unit	Lithostratigraphic Unit	Lithologic Description
Holocene		Surfical Aquifer System	Undifferentiated Pleistocene-Holocene Sediments	Fine-to-coarse grained, poorly-indurated quartz sands with minor amounts of clay
Pleistocene				
Pliocene				
Miocene		Confining Unit with lenses of the Intermediate Aquifer	Hawthorn Group	Interbedded siliciclastic-carboante sequences with occasional phosphate-rich units.
Oligocene		Upper Floridan Aquifer	Suwannee Limestone	Vuggy and muddy limestone
Eocene	Upper		Ocala Limestone	Fossiliferous limestone interbedded with vuggy, dolomitic limestone
	Middle		Avon Park Formation	Limestones and dolomites with interbedded evaporites in lower portion
	Lower		Oldsmar Formation	Gypsiferous limestone interbedded with gypsiferous dolomite
Paleocene			Lower Confining Unit	Cedar Keys Formation

Fig. 1. Lithostratigraphic and hydrostratigraphic units of the Santa Fe River Basin. Thickness of units not implied in the diagram. Modified from Miller (1986), Scott (1988), and Martin and Dean (2001).

thorn Group to the northeast, comprised in part of Miocene and younger siliclastic-dominated rocks (Scott, 1988; Groszos et al., 1992), and is unconfined in the southwest where the confining unit has been removed by erosion (Fig. 2). The erosional edge of the Hawthorn Group is referred to as the Cody Scarp (Puri and Vernon, 1964). To the northeast of the scarp, surface water is common on the confining unit, but is limited to the southwest where streams crossing the scarp either become losing streams, sink underground and reemerge, or disappear underground with no clear point of reemergence.

The Santa Fe River flows westward from Lake Santa Fe for about 40 km until it reaches the Cody Scarp, where it sinks into a 36-m deep sinkhole at the River Sink in O’Leno State Park (Fig. 2). The river flows underground through a network of conduits until it re-emerges about 6 km from the River Sink as a first-magnitude spring, called the River Rise, marking the headwaters of the lower Santa Fe River (Martin and Dean, 2001). The conduits rise to the surface intermittently between the River Sink and River Rise at several karst windows (Fig. 2).

At the Santa Fe Sink-Rise system, the UFA is about 430 m thick, unconfined at the surface, and is covered by a thin veneer (about 4 m, depending on land-surface elevation) of unconsolidated sediments (Miller, 1986). In this area, Oligocene carbonate rocks are

absent and no middle confining unit exists, resulting in the UFA extending from the Upper Eocene Ocala Limestone to the lower confining unit of the Lower Eocene Cedar Key Formation (Miller, 1986) (Fig. 1). Potable water extracted from the aquifer is estimated to come from the upper 100 m of the Ocala Limestone, with more mineralized water in deeper portions of the aquifer (Hunn and Slack, 1983; Miller, 1986). Porosity and matrix permeability of the Ocala Limestone average about 30% and 10^{-13} m^2 , respectively (Budd and Vacher, 2004; Florea, 2006). Exploration of the submerged conduits upstream of the River Rise has resulted in over 15 km of surveyed passage (Poucher, 2007). Average dimensions of the conduits range from 18 to 24 m wide and 12 to 18 m high with an average depth of about 30 m below the ground surface (mbgs) (Screaton et al., 2004; Poucher, 2007). The conduit system has not been completely mapped from the River Sink to River Rise, but high flow rates detected by natural and artificial tracers show the two locations are linked by conduits (Hisert, 1994; Martin and Dean, 1999; Moore and Martin, 2005).

Previous work has shown that water discharging from the River Rise varies between sources from the River Sink and from groundwater, defined here as water stored in the aquifer surrounding the conduits (e.g., Martin and Dean, 2001; Screaton et al., 2004; Martin et al., 2006). During high flow, discharge at the River Rise is mostly

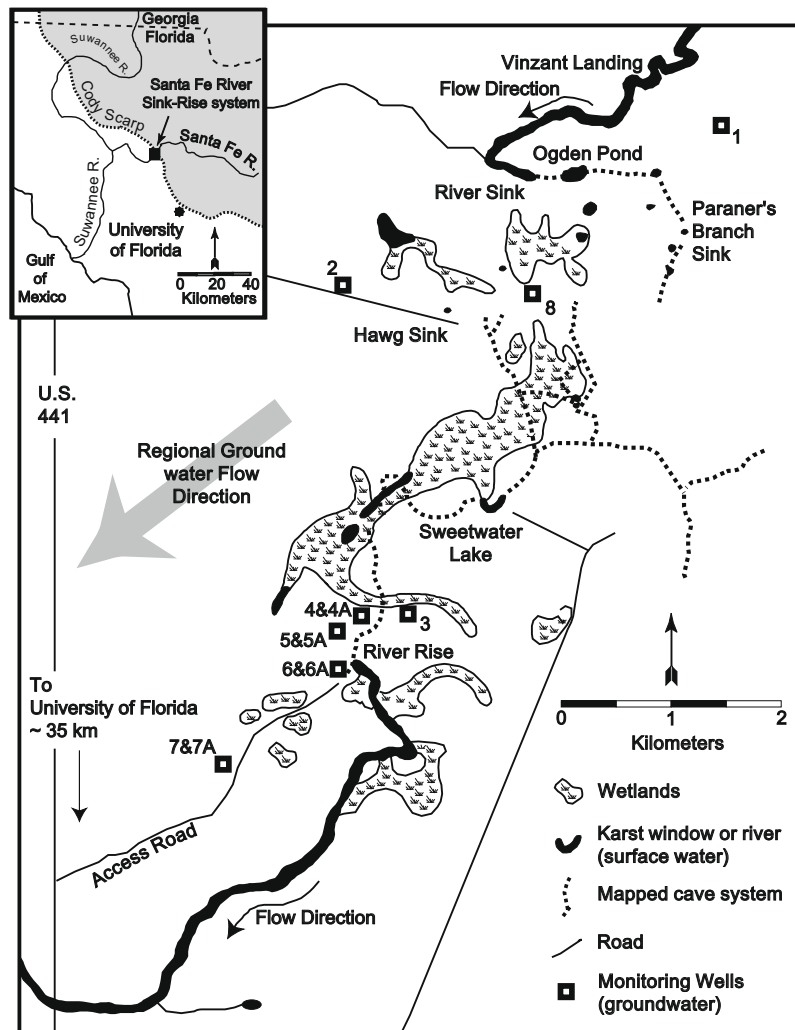


Fig. 2. Site location of the Santa Fe Sink-Rise system showing locations of surface water and groundwater sampling sites. Insert map shows location of Santa Fe Sink-Rise system in relation to north-central Florida. Dotted line represents erosional edge of the Hawthorn Group to the northeast (gray area) marking the confined portion of the Upper Floridan Aquifer, with the white area representing the unconfined portion of the UFA where the Hawthorn is absent.

derived from water entering the conduit system at the River Sink. As river stage and input into the River Sink decrease, increasingly larger percentages of groundwater drain from the surrounding aquifer into the conduit system to discharge at the River Rise (Martin and Dean, 2001).

Methods

River stage and potential recharge

Stage of the Santa Fe River was monitored about 200 m downstream of the River Rise with an automatic pressure transducer with an accuracy of ± 0.03 m. A separate barometric data logger (± 0.0045 m) was used for barometric compensation of the non-vented transducer. The water levels were recorded at 10-min intervals, and the data were downloaded from the recorder at 4- to 5-week intervals. When the data were downloaded, the river stage was measured from a staff gauge, and the recorded water level was referenced to the gauge for each download period to correct for drift. The relationship between stage and discharge at the River Rise was calculated based on the rating curve developed by Sreaton et al. (2004), using data collected by the Suwannee River Water Management District (SRWMD). Potential recharge was estimated as precipitation minus evapotranspiration ($P - ET$) during the study period by Ritorto et al. (2009). Briefly, daily values of $P - ET$ are estimated using daily precipitation data collected in O'Leno State Park using an automated rain gauge maintained by SRWMD (<http://www.srwmd.state.fl.us/index.asp?NID=99>), and the Penman–Monteith model for estimating daily ET, which estimates water loss to the atmosphere from a vegetative surface (Dingman, 2002).

Field sampling and laboratory analysis

Sixteen sampling trips were conducted from January 2003 to April 2007 to collect water from eight groundwater monitoring wells, one sinking stream (River Sink), one first-magnitude spring (River Rise), and four intermediate karst windows (Fig. 2). Monitoring wells were drilled to depths of about 30 mbgs, approximately at the depth of the conduits, and screened over 6-m (20 ft) depth intervals using 250 μ m PVC screening material attached to 51 mm (2 in.) diameter PVC linear. Groundwater samples were collected from monitoring wells using a Grundfos II submersible pump. Surface-water samples were collected on shore with a peristaltic pump attached to tubing that was pushed close to spring boils when visible, or in the deepest part of the sinkhole if no boil was present. Field measurements of temperature (T), pH, and specific conductivity (SpC) were recorded with a YSI multiprobe model 556 prior to sampling. The probe was calibrated at the start of each sampling day, and calibration was checked several times while in the field. All samples were collected unfiltered in high density polyethylene (HDPE) bottles. Samples collected for cations were preserved with either sulfuric (Na^+ and K^+) or nitric acid (Ca^{2+} and Mg^{2+}) to a pH < 2.0, while samples for anions and alkalinity were collected with no preservatives. Samples were stored on wet ice until they were delivered to the laboratory for analysis.

Concentrations of major ions (Na^+ , K^+ , Ca^{2+} , Mg^{2+} , Cl^- , and SO_4^{2-}) and alkalinity were analyzed by a NELAC-certified laboratory, Advanced Environment Laboratories, Inc., in Gainesville, FL. Analyses were determined in accordance with Environment Protection Agency (EPA) regulations for each analyte (EPA, 1983). Data from quality-assurance samples indicate no contamination resulted from sampling procedures and equipment, and that good analytical reproducibility occurred in the laboratory. Charge balance errors

for most samples were $\pm 5\%$ except for samples whose concentrations were near instrument detection limits.

Principal component analysis

Principal component analysis (PCA) is a multivariate statistical technique used to reduce the complexity of and decipher patterns within large data sets by determining a small number of variables that account for the greatest variance in all of the original variables (Wold et al., 1987; Jolliffe, 2002). For this study, PCA was applied to a normalized data matrix of nine variables (river stage, pH, Cl^- , SO_4^{2-} , Ca^{2+} , Na^+ , Mg^{2+} , K^+ , and alkalinity concentrations) from 211 water samples using the *princomp* function in MATLAB (Statistics toolbox 5.0, Mathworks, Waltham, MA). Because our data have large ranges and different units of measurement (e.g., stage and concentration), the data were normalized by centering the data set about zero by subtracting the means of each variable set from the measured value for individual samples and dividing each value within the variable set by its standard deviation (Stetzenbach et al., 1999; Chen et al., 2007). Consequently, each variable was normalized to unit variance and thus contributes equally to the analysis.

Principal components (PC) are eigenvectors of the correlation matrix of the normalized data set, and represent correlation coefficients, called loadings, between each variable and each PC. Since the correlation matrix is symmetrical, the eigenvectors are orthogonal and thus each PC is projected as an uncorrelated axis in a new space that helps explain the relationship among data points or variables along each PC. Positive loadings show a direct relationship, and those with the strongest absolute magnitude exert the greatest influence on the PC. The first PC accounts for the greatest fraction of variance of the correlation matrix, followed by subsequent components reflecting less variance. Principal component scores are transformed data points projected into PC space by axis rotation and correlating the weight of each loading variable to the original, normalized data. By plotting PC scores, similarities and disparities can be observed between the samples. For example, PC scores that cluster show their variance results from similar variable loadings, and thus suggest similar processes influence the samples. Furthermore, PC scores that vary along linear trends suggest variable loadings that affect these samples may exhibit some systematic variations such as, in this case, through time or with changing stage. In contrast, dissimilar PC scores show samples that are unrelated, likely suggesting these samples are influenced by independent processes.

Estimate of vertical flow rate from temperature perturbations

Upwelling of deep-water can be estimated assuming vertical flow within the UFA drives heat transfer following one-dimensional steady-state flow described by

$$\frac{\partial^2 T_z}{\partial z^2} - \left(\frac{c_w \rho_w v_z}{k} \right) \left(\frac{\partial T_z}{\partial z} \right) = 0, \quad (1)$$

where T_z is temperature at depth z , ρ_w is density of water, c_w is heat capacity of water, v_z is vertical Darcy velocity of water (positive for downward flow and negative for upward flow), k is thermal conductivity of the porous material (Bredehoeft and Papadopoulos, 1965). With boundary conditions of T_0 as the uppermost T at $z = 0$ and T_L as the lowermost T at $z = L$ yields a solution to Eq. (1) for T_z of

$$T_z = T_0 + (T_L - T_0) \left(\frac{\exp\left(\beta \left(\frac{z}{L}\right)\right) - 1}{\exp(\beta) - 1} \right), \quad (2)$$

(Bredehoeft and Papadopoulos, 1965), where L is the thickness of the vertical section and β is the dimensionless Peclet number for heat transfer

$$\beta = \frac{\rho_w c_w v_z L}{k} \quad (3)$$

Rearranging Eq. (3) for v_z yields an expression for the vertical flow rate of

$$v_z = \frac{k\beta}{\rho_w c_w L} \quad (4)$$

Results

River stage and P – ET

Average river stage during the entire study period was 10.2 masl with an average discharge of about 16 m³/s (Fig. 3). Samples collected during trips S-2, S-9, and S-11 occurred during high flow events when the river was above average stage. All other samples were collected during average or low flow.

Within the study area, changes in river stage appear to correlate positively over long time periods with P – ET, but this relationship seems to breakdown for individual events suggesting that antecedent conditions are important to river stage and discharge (Fig. 3). Between January 2003 and April 2007, average annual P – ET was about 400 mm (Ritorto et al., 2009). The maximum annual P – ET of about 990 mm occurred in 2004 due to an active hurricane season (see Florea and Vacher, 2007), which resulted in the highest stage of 14.1 masl. This high stage occurred immediately after Hurricane Frances delivered a total of 400 mm of P – ET to O'Leno State Park over a 6-day period in September 2004 (Fig. 3). The lowest stage of 9.6 masl occurred in April 2007 following a year-long drought that resulted in the area receiving a total of 83 mm of P – ET.

In addition to long-term events affecting stage, short-duration storms that exceed ET also cause variable responses in river stage, but these events did not cause a systematic response in the river (Fig. 3). Six rain events that produced a total of 232 mm of P – ET over a 39-day period in February and March 2003 caused a 3-m rise in river stage on March 13, 2003. In February 2004, about half of the P – ET in February and March 2003 (144 mm) produced only a tenth of the increase in river stage (0.33 m) seen the previous year. Conversely, only about 82 mm of P – ET over an 11-day period in March 2005 resulted in a 1.8-m rise in river stage on March 30, 2005.

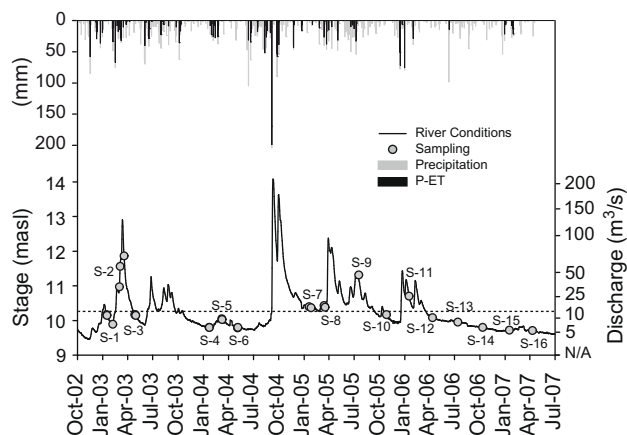


Fig. 3. Stage and discharge of the Santa Fe River at the River Rise, and precipitation and potential recharge (precipitation minus evapotranspiration; P – ET) amounts estimated within O'Leno State Park. Gray dots represent times of sample collection. Dashed line represents average stage (10.2 masl) during study period.

Water temperature and chemistry

Temperature of the water at the surface water sites vary depending on the air temperature (e.g., Martin and Dean, 1999), but temperature of the groundwater is more consistent, although variable among the wells. Temperatures at all wells, except Well 2, averaged around 21 °C with small variations between sampling times (Table 1). These measured temperatures are similar to average air temperature in the region as well as the typical temperature of water discharging from the regional springs (Hunn and Slack, 1983). In contrast, water temperatures are higher and more variable at Well 2 than all other wells, ranging from about 22 to 26 °C, with the highest temperature measured following a 1-year drought.

The chemical variations from two surface-water sites (River Sink and River Rise) and three groundwater wells (Wells 2, 4, and 7) are shown in a Piper diagram (Fig. 4). A statistical summary of the major chemistry is shown in Table 1. These five sites show the greatest variation in water chemistry, and all of the other sites that were sampled during the study (data not reported here) have chemical compositions similar to one of these five sites. These five sites are thus used to represent the continuum of water chemistry across the region (Fig. 4). The variation in water chemistry reflects three end-member sources that develop two mixing trends. One trend extends from one end-member characterized by a Ca–HCO₃ composition (① in Fig. 4) to another with Ca²⁺ and Mg²⁺ as the primary cations, but with more SO₄²⁻ and less HCO₃⁻ as the charge-balancing anion (② in Fig. 4). The composition of Well 4 reflects the Ca–HCO₃-type end-member. Water from Well 2 has a chemical composition reflecting a strong influence from the Ca–Mg–SO₄-type end-member, although the high coefficient of variation (CV) of major-element concentrations, SpC, and T suggests contributions of this end-member are variable at this site (Table 1). For example, SpC and T at Well 2 range from 488 to 1315 μS/cm and 22 to 26 °C, respectively. Well 7 falls along the mixing trend between Wells 4 and 2, suggesting it may be influenced by both sources of water (Fig. 4).

The third end-member is characterized by elevated concentrations of Na⁺ and Cl⁻, and occurs at the River Sink at high flow (③ in Fig. 4). This end-member develops a second mixing trend that is confined to water collected from the surface-water sites, but this trend reflects extensive mixing between all three end-members. During certain sample trips (e.g., S-3, S-4, S-6, S-10, and S-12 through S-16), water from the River Sink and River Rise fall along the mixing line between Wells 4 and 2, reflecting little influence from the Na–Cl-type end-member (Fig. 4).

Principal component analysis

Principal component analysis identifies which of the measured components provide the greatest variation in the composition of the water (e.g., Stetzenbach et al., 1999; Stetzenbach et al., 2001; Chen et al., 2007; Fournier et al., 2007). The first three PCs (eigenvalues of 4.87, 2.13, and 1.16, respectively) explain a total of 91% of the variance, or 54%, 24%, and 13%, respectively (Table 2). When PCs 1 and 2 are considered together, differences in the loadings are represented by two clusters and one outlier (Fig. 5A). One cluster shows a strong positive loading (loading > 0.3: bold font Table 2) of Na⁺, Mg²⁺, K⁺, Cl⁻, and SO₄²⁻ on PC 1. While these components carry similar weights on PC 1, only K⁺ also has a strong positive loading on PC 2 followed by weaker positive loadings of Cl⁻ and Na⁺. Although SO₄²⁻ and Mg²⁺ are heavily loaded on PC 1, they show no loading on PC 2. The other cluster of pH, alkalinity, and Ca²⁺ has a weak positive loading on PC 1 and a strong negative loading on PC 2. The single variable that plots as an outlier in Fig. 5A is river stage, which has a weak negative loading on PC 1 and a strong po-

Table 1
Summary of major ions, alkalinity, SpC, pH, and *T* of representative water samples.

Location		River Sink	River Rise	Well 2	Well 4	Well 7
Cl	Range	0.226–0.643	0.319–0.643	0.423–1.66	0.226–0.282	0.279–0.536
	<i>x</i>	0.386	0.468	1.24	0.247	0.420
	CV	27	17	28	6	18
SO ₄	Range	0.021–0.485	0.021–1.15	1.19–4.47	0.021–0.052	0.024–0.285
	<i>x</i>	0.236	0.626	3.43	0.042	0.159
	CV	69	61	28	18	38
Ca	Range	0.190–1.39	0.203–2.02	1.97–4.77	2.07–2.36	1.54–2.77
	<i>x</i>	0.781	1.24	3.92	2.21	2.19
	CV	58	55	18	3	19
Na	Range	0.196–0.457	0.244–0.518	0.613–1.61	0.183–0.221	0.192–0.335
	<i>x</i>	0.301	0.386	1.26	0.200	0.272
	CV	19	23	23	6	17
Mg	Range	0.095–0.642	0.095–0.716	0.568–2.04	0.051–0.090	0.152–0.238
	<i>x</i>	0.347	0.437	1.48	0.058	0.179
	CV	58	54	32	16	13
K	Range	0.020–0.047	0.024–0.041	0.035–0.082	0.005–0.010	0.015–0.023
	<i>x</i>	0.028	0.027	0.060	0.009	0.019
	CV	27	15	28	14	13
Alkalinity	Range	0.16–3.04	0.16–3.16	2.04–4.28	2.80–4.30	2.16–5.12
	<i>x</i>	1.56	1.90	3.89	4.03	4.12
	CV	71	58	13	9	19
pH	Range	5.40–7.79	4.70–7.37	6.48–7.10	6.48–7.19	6.50–7.40
	<i>x</i>	6.94	6.90	6.84	6.87	6.95
	CV	9	9	3	3	4
SpC	Range	73.0–412	72.5–560	488–1315	390–449	306–550
	<i>x</i>	256	371	1058	428	434
	CV	48	46	20	3	20
<i>T</i>	Range	10.0–27.7	11.0–26.4	22.0–26.3	20.9–21.7	20.3–20.9
	<i>x</i>	19	20	25	21	21
	CV	27	20	4	1	1

Range and mean (*x*) of concentrations in mmol/kg H₂O, coefficient of variation (CV) in %, SpC in μS/cm, pH is unitless, and *T* in °C.

sitive loading on PC 2. When PC 2 and PC 3 are considered together, a strong inverse relationship exists between the pH and river stage, suggesting that these two components are responsible for most of the 13% variance on PC 3, since Ca²⁺ has similar loadings on both PC 2 and PC 3 and alkalinity remains negatively loaded on PC 3 although less on PC 2 (Table 2).

The PC scores for each sample are calculated as the sum of the PC loading times the normalized values for that sample, e.g.,

$$\begin{aligned} \text{PC 1 score} = & 0.08 (\text{pH}) + 0.42 (\text{Cl}) + 0.44 (\text{SO}_4) + 0.27 (\text{Ca}) \\ & + 0.44 (\text{Na}) + 0.44 (\text{Mg}) + 0.39 (\text{K}) \\ & + 0.05 (\text{alkalinity}) - 0.10 (\text{stage}). \end{aligned} \quad (5)$$

These values thus represent the relative influence each loading has on the water sample for a given PC. While all surface- and groundwater sites were included in the PCA, only sites that reflect the greatest variation in water chemistry and most closely define the end-member compositions (i.e., those sites shown on Fig. 4) are plotted in Fig. 5B.

The advantage of plotting PC scores in this fashion over using Piper diagrams is that the variation in samples can be observed at a higher resolution, thereby revealing additional information and relationships previously unrecognized (e.g., Melloul and Collin, 1992; Laaksoharju et al., 1999; Olofsson et al., 2006). For example, the strong positive loading of K⁺ on both PC 1 and PC 2 suggests multiple sources of K⁺, such as dissolution of K-bearing minerals, application of fertilizers to the land surface, and seawater. This information is masked in the Piper diagram because Na⁺ and K⁺ are grouped together during ion balancing. Although samples from Wells 2, 4, and 7 lie along the mixing trend between the Ca–HCO₃ and Ca–Mg–SO₄-type end-members in the Piper diagram (Fig. 4),

their projection in PC space allows observations of additional relationships and disparities (Fig. 5B). For example, water from Wells 4 and 7 have slightly negative PC 1 scores with minimal variability, but show greater variability on PC 2. Conversely, water from Well 2 is highly variable on both PC 1 and PC 2 scores with the strongest positive PC 1 scores of any water sampled. In addition to the groundwater samples, surface-water samples from the River Sink and River Rise show some variance on PC 1, which are scattered and overlap each other on the negative side, but separate into two distinct groups on the positive side. Most of the variance in these samples occurs on the positive side of PC 2, which relates directly with stage and inversely with loadings of pH, alkalinity and Ca²⁺.

Discussion

Temporal variations in spring discharge and chemistry have often been used to understand groundwater flow paths and sources of recharge in both telogenetic and eogenetic aquifers because springs are commonly assumed to reflect processes that occur over large scales and may be the only point of access to the groundwater (e.g., Shuster and White, 1971; Dreiss, 1989; Katz, 2004; Vesper and White, 2004; Toth and Katz, 2006). Recent studies, however, suggest monitoring the spatial and temporal variations in groundwater may elucidate additional aquifer parameters unrecognized by only monitoring karst springs (Scanlon, 1989; Martin and Dean, 2001; Toran et al., 2007). In the following section, we use representative end-member water types to describe the sources of water to the sink-rise system, followed by a mass-balance calculation to estimate the relative contribution each source provides to spring discharge at the River Rise. Comparison of these results to physical conditions, including river stage, precipitation, and ET, provides in-

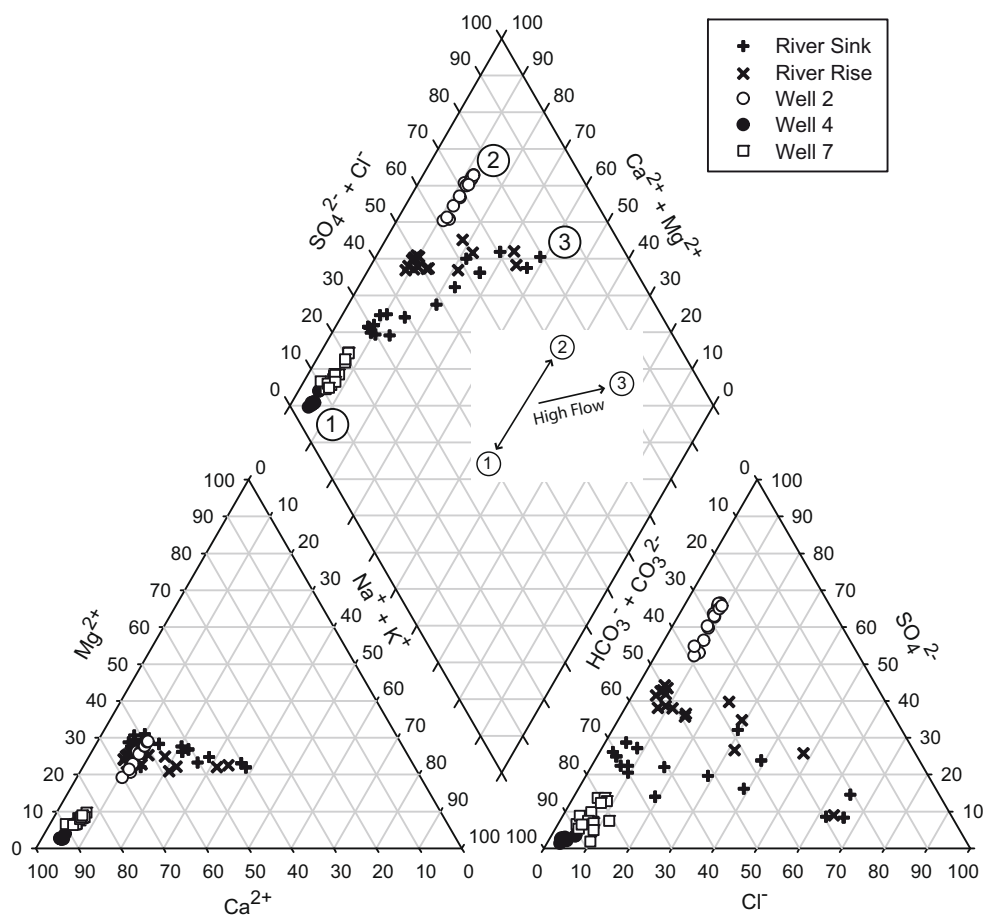


Fig. 4. Piper diagram showing the hydrochemical facies of surface and groundwater in Santa Fe Sink-Rise system. Representative end-members are (1) Ca–HCO₃ type water; (2) Ca–Mg–SO₄-type water; (3) Na–Cl-type water. Inset in diamond shows mixing trends between the three end-members.

Table 2
PCA variable loadings.

Variables	Loadings ^a		
	PC 1	PC 2	PC 3
pH	0.08	–0.42	0.53
Cl	0.42	0.15	0.00
SO ₄	0.44	0.00	–0.07
Ca	0.27	–0.46	–0.39
Na	0.44	0.07	–0.02
Mg	0.44	0.02	0.07
K	0.39	0.31	0.09
Alkalinity	0.05	–0.62	–0.36
Stage	–0.10	0.32	–0.65
Eigenvalues	4.87	2.13	1.16
% Variance	54	24	13
% Cumulative	54	78	91

^a Loadings greater than |0.3| are in bold.

sight to the complex nature of the aquifer that could be overlooked if aquifer characteristics were determined only by monitoring the spring. This analysis illustrates the importance of coupling groundwater monitoring, physical conditions, and spring discharge and chemistry when interpreting the physical and chemical characteristics of karst aquifers.

End-member chemistry and sources of water

Allogenic recharge

When PC loadings and scores are considered together, the source of water entering the River Sink has a statistical association

with stage (Fig. 5). Positive loadings of stage, K⁺, Na⁺, and Cl[–] and negative loading of pH, Ca²⁺, and alkalinity on PC 2 suggest allogenic recharge at the River Sink delivers increasing concentrations of K⁺, Na⁺, and Cl[–], but dilutes pH, Ca²⁺, and alkalinity as stage increases (Fig. 5A). These relationships indicate that water entering the River Sink during high flow is evolved rain water flowing overland or in the shallow subsurface during storm events with minimal groundwater contribution (cf. Sklash and Farvolden, 1979). The evolved rain water accounts for the Na–Cl-type end-member (3) in Fig. 4, which has an average Na⁺/Cl[–] ratio of 0.81 ± 0.19 (1σ), close to the 0.86 ratio of seawater.

Seawater could be an important contribution to major-element chemistry with positive loading on PC 2 (Na⁺, Cl[–], and K⁺), although other factors such as introduction of contaminants and reactions with siliciclastic minerals in the confining Hawthorn Group also could be important. Seawater would be the primary source of Na⁺ and Cl[–] to the region as sea spray becomes entrained in precipitation when tropical storms and summertime convective thunderstorms move inland from the coast. Some of the water has Na⁺/Cl[–] ratios in excess of seawater values, which may reflect excess Na⁺ due to leaching of soil particulates in the atmosphere (Junge and Werby, 1958) or due to cation exchange in the siliciclastic Hawthorn Group (Rose, 1989). Cation exchange could also remove Na⁺ from the water, which would explain the Na⁺/Cl[–] ratios that are below seawater value. Potassium is unlikely to be derived only from sea spray since the average K⁺/Cl[–] ratio of 0.08 ± 0.02 (1σ) exceeds by a factor of four the 0.02 ratio of seawater. Although K⁺ could result from dissolution of K-bearing minerals in the Hawthorn Group (Edwards et al., 1998), these minerals occur in trace

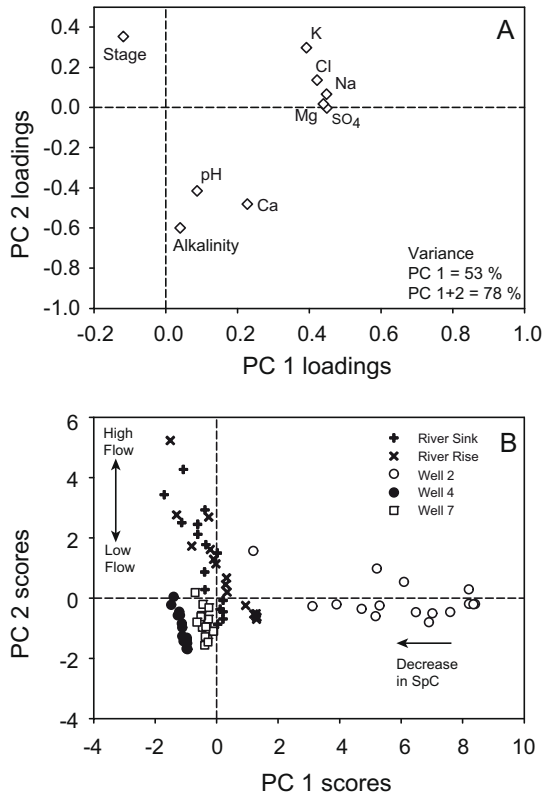


Fig. 5. (A) Plot of PC loadings for major ions, alkalinity, pH, and river stage and (B) plot of PC scores for River Sink, River Rise, and Wells 2, 4, and 7.

amounts that would unlikely provide the observed concentrations. The elevated concentration of K^+ in allogenic water, as reflected by its strong positive loading on PC 2 (Fig. 5A), probably results from leaching of artificial fertilizers used for agriculture (Katz et al., 2001; Chelette et al., 2003).

The negative loadings of pH, Ca^{2+} , and alkalinity on PC 2 reflect dilute rainwater entering the River Sink during high flow. In these conditions, pH values are lower than would be expected for water buffered by dissolution of carbonate minerals, and mineral sources of Ca^{2+} and alkalinity (e.g., HCO_3^-) are scarce in upper sections of the Hawthorn Group (Scott, 1988). Although middle portions of the Hawthorn Group contain limestone and dolostone units (Groszos et al., 1992), the negative loadings of Ca^{2+} and alkalinity and no loading of Mg^{2+} on PC 2 (Fig. 5A) suggest allogenic recharge has not interacted with these carbonate minerals. Sulfate also shows no statistical association with stage on PC 2 (Fig. 5A), suggesting this water has not dissolved mineral sources of S, such as gypsum, anhydrite, or pyrite, which exist in minor amounts throughout the Hawthorn Group (Lazareva and Pichler, 2007).

During times of little precipitation, river stage drops as lesser amounts of runoff from the confined area contribute to river flow, and water at the River Sink trends towards an intermediate composition between the two groundwater end-members (① and ② in Fig. 4). This mixing between the three end-members is observed in the PCA where River Sink scores on PC 2 shows a strong positive association with stage during high flow, but become negative during low flow as loadings of pH, Ca^{2+} , and alkalinity exert a stronger influence on the composition of allogenic water (Fig. 5). These relationships suggest that, during low flow conditions, water at the River Sink is a mixture of allogenic runoff and groundwater from the UFA, which has a different composition than water entering the River Sink during high flow. Consequently, water entering the UFA through swallets may be time-dependent mixtures of water

that originates from the surface or the surrounding aquifer depending on conditions such as river stage, precipitation, and ET.

Groundwater

The differences in chemical compositions between water from Wells 2 and 4 reflect two distinct sources (Fig. 4). Well 4 has $Ca-HCO_3$ -type water similar to most shallow groundwater of the UFA and results from rain water equilibrating with the Ocala Limestone (Sprinkle, 1989). Although Well 4 is located only about 100 m from the conduit, its variation on PC 2 scores shows no statistical association with stage (Fig. 5B). Most of the variation of Well 4 on PC 2 scores likely results from subtle changes in pH, Ca^{2+} , and alkalinity, whose loadings exert the greatest influence on the $Ca-HCO_3$ -type water (Fig. 5B). Water at Well 4 is likely to originate from diffuse recharge as indicated by the small variations in solute/ Cl^- ratios (Fig. 6A). The magnitude of diffuse recharge has been shown to exceed allogenic recharge at the River Sink depending on conditions including ET, soil saturation, and precipitation (Ritorto, 2007).

The $Ca-Mg-SO_4$ -type water from Well 2 results from processes other than, or in addition to, simple limestone dissolution. Although all wells are screened at similar depths below the land surface, water collected from Well 2 is the most mineralized in the region with the highest major-element concentrations and SpC. Well 2 also has the highest T of all water collected (Table 1). Consequently, the positive loadings of K^+ , Cl^- , Na^+ , Mg^{2+} , and SO_4^{2-} on PC 1, coupled with the strong positive PC 1 scores of Well 2, suggest this water source delivers most of these ions to the sink-rise system (Fig. 5). Water with similar SO_4^{2-} concentrations (in excess of 400 mg/l, i.e. about 4.2 mmol/kg H_2O) was previously observed from a municipal well in High Springs, FL (less than 5 km from Well 2) that was open to the UFA from about 105 to 150 mbsg (Hunn and Slack, 1983). The nearby presence of deep, mineralized

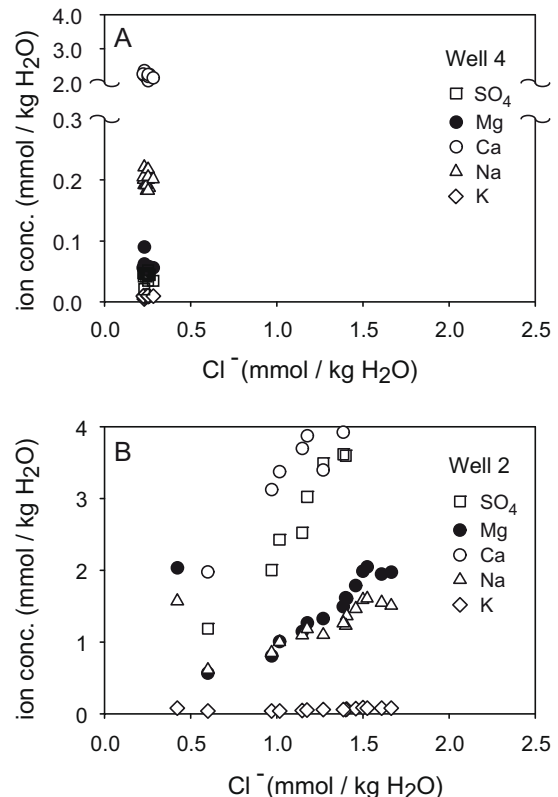


Fig. 6. Plots of ion concentrations versus Cl^- at (A) Well 4 and (B) Well 2.

water could reflect a source of water that would give Well 2 its unique chemical composition. While the source of mineralized water deep within the Floridan aquifer system has not been determined (e.g., Phelps, 2001), the increased salt contents cannot result from only mixing with seawater. Comparing ratios of dissolved components to Cl^- concentrations to their seawater values suggests the mineralized water at Well 2 has concentrations of Mg^{2+} and SO_4^{2-} that exceed values expected from seawater fractions by a factor of 11 and 49 times, respectively, and the average Na^+/Cl^- ratio of 0.96 ± 0.06 (1σ) (Table 1) at Well 2 is about 10% higher than the seawater value. Nonetheless, elevated concentrations of K^+ at Well 2, as reflected by its strong positive loading on PC 1 (Fig. 5A), suggests dilute seawater deep within the aquifer may account for some of the mineralized water since this is the likely source of K^+ in the UFA (Sprinkle, 1989).

Other than seawater as a source of salts at Well 2, water–rock reactions could provide its elevated ion concentrations. Elevated concentrations could result from water reacting with minerals in leaky portions of the Hawthorn Group, which then moves along deep flow paths due to regional head gradients (Lawrence and Upchurch, 1982; Wicks and Herman, 1994; Katz et al., 2004). An alternate explanation for the elevated concentrations could result from evaporite dissolution and dedolomitization occurring deep within the aquifer (e.g., Plummer, 1977; Hanshaw and Back, 1979; Jones et al., 1993). In the lower portions of the UFA, evaporite minerals and dolomite are known to occur (Miller, 1986) (Fig. 1). Dissolution of gypsum or anhydrite releases Ca^{2+} and SO_4^{2-} , which initiates calcite precipitation and subsequently promotes additional dissolution of gypsum or anhydrite and dolomite if present (Plummer and Back, 1980).

Although near-surface reactions in the Hawthorn Group could elevate ion concentrations in the UFA, dissolution of evaporite minerals and dolomite in deeper portions of the aquifer are likely responsible for the observed concentrations at Well 2. These processes would elevate concentrations of SO_4^{2-} , Mg^{2+} , and Ca^{2+} , but would not increase the concentration of K^+ (Fig. 6B). Dissolution of Ca-bearing minerals, however, would not explain the linearity between Na^+ and Cl^- or the value of Na^+/Cl^- molar ratio of 0.96 ± 0.06 (1σ), which is similar to the Na/Cl molar ratio of halite and suggest halite dissolution although no halite has been reported in the Floridan Aquifer system (Miller, 1986).

Influence of vertical flow on shallow-water chemistry

Most work on groundwater flow at our study site and other karst systems has focused on horizontal flow through conduits and surrounding aquifer following rapid recharge through swallets and discharge from springs (Katz et al., 1998; Crandall et al., 1999; Martin and Dean, 2001; Screaton et al., 2004). Few studies have considered vertical flow through karst aquifers or the geographic distributions and controls of where vertical flow could occur (e.g., Jones et al., 1993; Sprouse, 2004). The chemical variations at Well 2, where measured temperatures are significantly higher than surrounding wells, indicate that upward flow is important in the region, which we estimate below using Eqs. (2) and (4) (Fig. 7). For T_z , we use a measured T of 26 °C at Well 2, which represents the highest T observed at Well 2 and occurred following a 1-year drought (S-15 and S-16, Fig. 3). The drought may have increased hydraulic head differences between the deep and shallow portions of the aquifer as drought conditions have greater effect on the shallower portions of the aquifer. In addition to head differences, the drop in river stage during the drought minimizes flow through conduits, thereby reducing horizontal flow which may also alter the T at the well (e.g., Lu and Ge, 1996).

Considering this conceptualization of vertical flow at Well 2, we estimate z and L to be 23 and 423 m, respectively, during this time

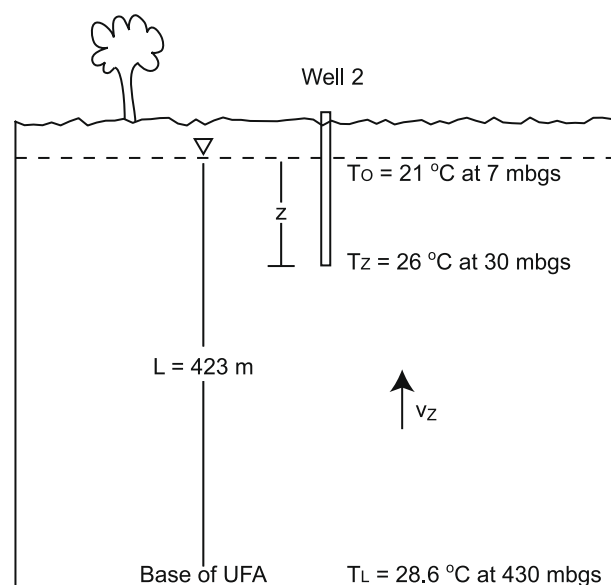


Fig. 7. Diagrammatic sketch of boundary conditions for vertical steady-state flow and heat transfer at Well 2.

(Fig. 7). Although there is no water-table well near Well 2, we estimate T_0 to be about 21 °C based on the average groundwater T (e.g., Wells 4 and 7, Table 1) and average air T for the area (Hunn and Slack, 1983). We estimate a temperature of 28.6 °C for T_L at the base of the UFA, assuming an average geothermal gradient of about 1.8×10^{-2} °C/m across the region (Reel and Griffin, 1971; Smith and Lord, 1997). Solution to Eq. (2) using these T values suggests β at Well 2 is about -19.6 . Using a heat capacity of 4184 J/kg °C, density of 1000 kg/m³ for water, and thermal conductivity of limestone of 3 W/m °C (Deming, 2002), Eq. (4) yields an upward Darcy velocity at Well 2 of about 1 m/year.

Although we observe the temperature anomaly resulting from vertical flow only at Well 2, the deep-water source appears to have a significant impact on the regional shallow-water chemistry as shown by the chemical compositions at Wells 2 and 7, River Sink, and River Rise. During low flow conditions, water at the River Sink and River Rise appear to be intermediate mixtures of the groundwater end-members (① and ② in Fig. 4), although water from the River Sink lies closer to the Ca–HCO₃-type end-member while the River Rise lies closer to the Ca–Mg–SO₄-type end-member (Fig. 4). This difference in water chemistry at low flow suggests the River Rise receives a greater contribution from the deep-water source than the River Sink.

Dilution of the deep-water source at Well 2 is shown by the variation in Well 2 scores on PC 1, which changes with SpC (Fig. 5B). As dilute allogenic water reaches Well 2, the concentrations of K^+ , Cl^- , Na^+ , Mg^{2+} , and SO_4^{2-} decrease, resulting in PC 1 scores plotting towards the graph's origin (Fig. 5B). These changes suggest that Well 2 is more closely linked to surface water than the other wells, possibly through unmapped conduits (Fig. 2). The deep-water source at Well 2 requires greater vertical permeability than the other wells. Higher permeability could result from vertical fractures that would provide a flow path for deep-water, and if these fractures are linked to the conduit sourcing the River Rise, could explain the greater influence of deep-water there than at the River Sink (Fig. 4). The only other location with a signal from the deep-water source is Well 7 (Fig. 4), but its location is about 1 km away from the closest known conduit (Fig. 2). Although simulations of regional groundwater flow suggest water upwelling from deep flow paths exert little influence on first-magnitude springs draining the UFA (Bush and Johnston, 1988), deep-water at the sink-rise

system suggests heterogeneous permeability can greatly alter groundwater flow fields and reflects the importance of multiple flow paths in karst aquifers (e.g., Knochemus and Robinson, 1996).

Effects of source water and flow paths on spring discharge

Volumes of allogenic and diffuse recharge have been estimated for the River Rise (e.g., Martin and Dean, 2001; Sreaton et al., 2004; Ritorto et al., 2009), but contributions from the deep source have not yet been included in water mass balance estimates although the chemical composition of the River Rise water indicates the deep source contributes to its discharge. Estimating the volume of deep-water sourcing the River Rise is difficult because of uncertainty in the chemical composition of the deep-water end-member. While chemical compositions of end-members represented by allogenic recharge and shallow sources can be measured directly at the River Sink and Well 4, respectively (e.g., Fig. 4), the composition of the end-member reflecting the deep-water source can not be directly sampled. Instead, water chemistry at Well 2 is a mixture of both deep and shallow-water, and consequently mass balance calculations can only approximate the relative fractions of water sourcing the River Rise. While dissolution and precipitation reactions within the conduit may affect spring composition to some degree, we assume the mixing of the three representative end-members largely accounts for most of the chemical variation at the River Rise (Figs. 4 and 5B).

We use concentrations of Mg^{2+} and SO_4^{2-} to estimate the relative fractions of the three sources of water discharging from the River Rise. Concentrations of Mg^{2+} and SO_4^{2-} show strong linear correlations at the River Sink, River Rise, and Well 2 (Fig. 8). The linear relationship suggests that concentrations are controlled by dilution, which is most likely to occur from mixing of allogenic recharge and the concentrated deep-water source as shown by the PCA (Fig. 5). In contrast to the deep-water source at Well 2, concentrations of Mg^{2+} and SO_4^{2-} of diffuse recharge at Well 4 are low, remain relatively constant, and have nearly the same ratio through time (see Figs. 6A and 8) suggesting this water is not affected by inputs of allogenic or deep-water. Although Well 4 does exhibit a linear trend on PC 2 scores (Fig. 5B), no systematic cause for the variation exists.

In order to observe how temporal variations in the magnitudes of sources affect spring discharge, water fractions were calculated using Mg^{2+} and SO_4^{2-} concentrations from each sample trip. Assuming contributions only from the three identified end-members, water at the River Rise consists of volumetric fractions of each end-member, X ,

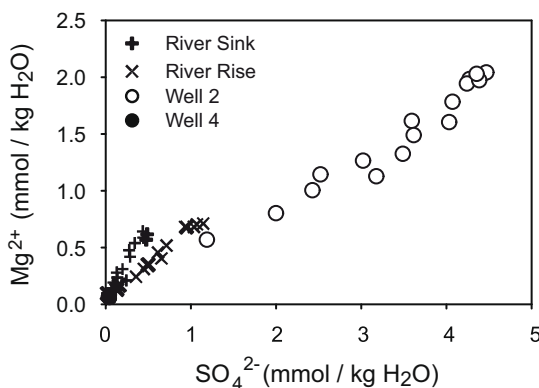


Fig. 8. Plot of Mg^{2+} versus SO_4^{2-} concentrations showing the temporal, linear variation at the River Sink, River Rise, and Well 2. Well 4 shows little change near the origin of the graph.

$$X_R = X_S + X_{W2} + X_{W4}, \quad (6)$$

where the subscripts represent allogenic recharge at the River Sink (S), the deep source at Well 2 (W2), diffuse recharge at Well 4 (W4), and discharge at the River Rise (R), which equals 1. Individual equations were written for Mg^{2+} and SO_4^{2-} concentrations where

$$X_R Mg_R = X_S Mg_S + X_{W2} Mg_{W2} + X_{W4} Mg_{W4} \quad (7)$$

$$X_R SO_{4R} = X_S SO_{4S} + X_{W2} SO_{4W2} + X_{W4} SO_{4W4}. \quad (8)$$

Rearranging Eq. (6) for X_S and substituting into Eq. (7) and solving for X_{W4} gives

$$X_{W4} = \frac{X_R (Mg_R - Mg_S) - X_{W2} (Mg_{W2} - Mg_S)}{Mg_{W4} - Mg_S}, \quad (9)$$

and rearranging Eq. (6) for X_{W4} and substituting into Eq. (8) and solving for X_S gives

$$X_S = \frac{X_R (SO_{4R} - SO_{4W4}) - X_{W2} (SO_{4W2} - SO_{4W4})}{SO_{4S} - SO_{4W4}}. \quad (10)$$

Substituting Eqs. 9 and 10 into Eq. (6) and solving for X_{W2} yields

$$X_{W2} = \frac{1 - \left(\frac{SO_{4R} - SO_{4W4}}{SO_{4S} - SO_{4W4}} \right) - \left(\frac{Mg_R - Mg_S}{Mg_{W4} - Mg_S} \right)}{1 - \left(\frac{SO_{4W2} - SO_{4W4}}{SO_{4S} - SO_{4W4}} \right) - \left(\frac{Mg_{W2} - Mg_S}{Mg_{W4} - Mg_S} \right)}. \quad (11)$$

Variables X_{W4} and X_S are found using back-substitution of solutions to Eq. (11) into Eqs. (9) and (10), respectively. Eqs. (9)–(11) provide the mixing fractions of source water contributing to discharge at the River Rise for all the sampling times except January 2003 (S-1, Fig. 3) prior to the installation of Well 4 (Table 3).

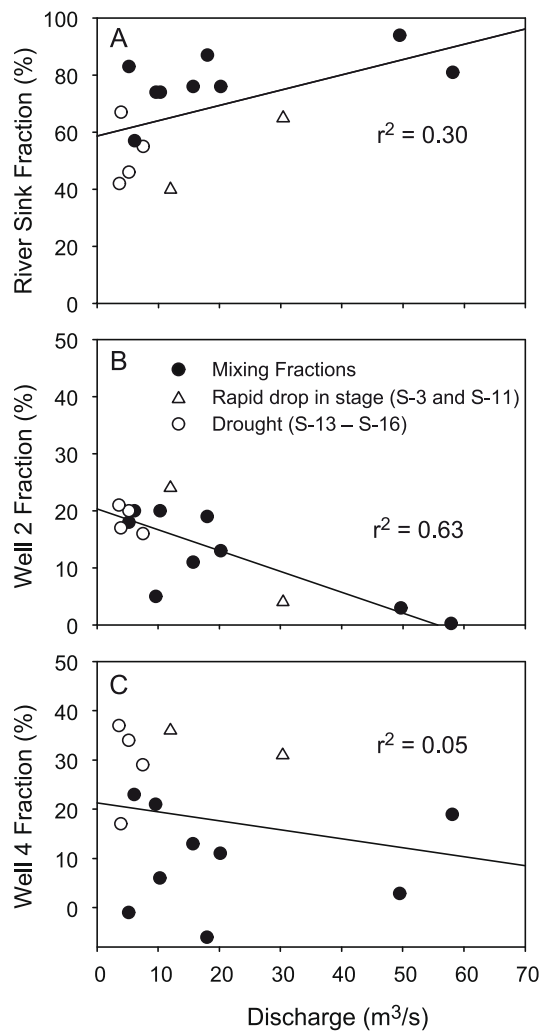
Results of the mixing calculations show that flow through the sink-rise system is quite complex. Nonetheless, discharge at the River Rise correlates positively, but weakly, with allogenic recharge (River Sink), inversely with the deep-water source (Well 2), but lacks a correlation with diffuse recharge (Well 4) (Fig. 9). These results agree with the PCA, which suggests that as allogenic recharge increases with stage the magnitude of the deep-water source decreases. This decrease in deep-water may reflect elevated head in the conduit limiting upward flow. The weak correlation of discharge and allogenic recharge may reflect time variations in chemical composition of the allogenic recharge depending on specific reactions. Differences in reactions would alter the allogenic water chemistry and the estimates of the percentage of diffuse recharge. The lack of correlation between discharge and diffuse recharge as represented by the Well 4 fraction (Fig. 9C) suggests that hydraulic head between the conduit and surrounding aquifer, and the related exchange of water between the conduit and matrix, do not change systematically with river stage. During times when diffuse recharge exceeds allogenic recharge, hydraulic head in the surrounding aquifer could exceed conduit head as diffuse recharge elevates the water table and causes flow from the matrix to the conduit and ultimately to discharge from the River Rise (Martin and Dean, 2001; Sreaton et al., 2004; Martin et al., 2006; Ritorto et al., 2009).

Certain sampling times provide information on how differences in hydraulic head between the conduit and surrounding aquifer may affect the chemical composition of water discharging from the River Rise. Prior to sampling on April 30, 2003 and January 17, 2006, river stage dropped rapidly, which would result in rapidly decreasing head in the conduit (indicated as Δ in Fig. 9). If head in the conduit dropped more quickly than head in the surrounding aquifer, pressure gradients would drive flow toward the conduit (Sreaton et al., 2004; Martin et al., 2006), decreasing the fraction of allogenic water to the River Rise and simultaneously increasing the fractions of matrix water. Consequently, these two sample times show the elevated fraction of water from Well 4 (diffuse recharge) relative to the River Sink fractions (allogenic recharge) (Fig. 9).

Table 3

Fraction of water discharging from the River Rise originating from the River Sink and two groundwater end-members.

Sample date	Sample period	Rise discharge (m ³ /s)	River Sink ^a (%)	Well 2 ^a (%)	Well 4 ^a (%)
3/2/03					
3/5/03	S-2	57.9	81	0	19
3/19/03					
4/30/03	S-3	12.0	40	24	36
1/23/04	S-4	5.2	83	18	-1
3/8/04	S-5	9.6	74	5	21
5/5/04	S-6	6.1	57	20	23
1/19/05	S-7	18.0	87	19	-6
3/18/05	S-8	20.2	76	13	11
7/18/05	S-9	49.5	93	3	3
10/27/05	S-10	15.7	76	11	13
1/17/06	S-11	30.4	65	4	31
4/12/06	S-12	10.3	74	20	6
7/13/06	S-13	7.5	55	16	29
10/10/2006	S-14	5.2	46	20	34
01/17/2007	S-15	3.9	67	17	17
04/10/2007	S-16	3.6	42	21	37

^a Percentages calculated based on solutions to Eqs. (9)–(11).**Fig. 9.** Plot of source contributions versus discharge at the River Rise from (A) River Sink; (B) Well 2; (C) Well 4.

During times of low flow, the conduit acts as a low-resistance drain that allows groundwater to converge on it (e.g., Freeze and Cherry, 1979; Ford and Williams, 2007). This process is observed during a drought from July 2006 to April 2007 (S-13–S-16, Fig. 3), when river stage constantly fell from about 10 to 9.7 masl,

far below the average stage of 10.2 masl. During this time, discharge from the River Rise was close to an even mixture of allogenic water (River Sink) and groundwater (Wells 2 and 4) (see ○ in Fig. 9). The fraction of deep-water (Well 2) was at a maximum, averaging around 20% of the total discharge, suggesting that first-magnitude springs draining the UFA may receive significant contributions of flow from upward movement from deep flow paths (e.g., Katz, 2004). The fraction of diffuse water (Well 4) is more variable than the fraction of deep-water, ranging from about 20 to 40%. This variability likely reflects changes in head gradient between the conduit and surrounding aquifer due to differences in antecedent conditions such as prior precipitation and ET. Variations in these factors would alter the elevation of the water table so that different amounts of matrix water would flow to the conduit for similar river stages (Fig. 3). Such processes could contribute to the weak correlation between allogenic recharge and discharge ($r^2 = 0.30$, Fig. 9A). Consequently, although matrix flow in unconfined eogenetic aquifers can provide significant amounts of spring discharge, its contribution through time at any one spring must be sensitive to processes affecting hydraulic head gradients between conduits and surrounding aquifer.

Conclusions

Spatial and temporal monitoring of surface- and groundwater chemistry along with observations of physical parameters including river stage, precipitation, and ET in the Santa Fe River Sink-Rise system of the eogenetic UFA provide insight on how multiple sources of water and several different flow paths may affect spring discharge in karst aquifers. Chemical monitoring and PCA suggest that mixing of two shallow sources (diffuse and allogenic recharge) and one upwelling deep-water source explains 91% of the chemical variation in the sink-rise system (Table 2). Deep-water sources within the UFA have been recognized previously, but our results are the first indication of a deep source at the Santa Fe River Sink-Rise system. This deep source provides most of Na⁺, Mg²⁺, K⁺, Cl⁻, and SO₄²⁻ to the system and thus is the primary influence on major-element chemistry. Estimates of vertical flow, based on maximum observed temperatures, are on the order of 1 m/year, and this flow appears to contribute up to 20% of the discharge at the River Rise. The contribution from the deep source depends inversely on flow conditions. The presence of a deep source suggests that care must be taken in the evaluation of karst aquifers based on the chemical composition of spring water, which may not be sourced only from shallow portions of the aquifer.

Water flowing through karst aquifers from allogenic inputs to springs should reflect an evolution of the recharged water by water–rock reactions along conduit flow paths. Comparison of relative fractions of source water, however, suggest the deep-water source and local diffuse recharge cause significant changes in the chemical composition of discharge even in a system dominated by allogenic recharge and conduit flow. While variations in spring chemistry likely reflect water–rock reactions along conduit flow paths between sinks and springs, mixing of different sources may play a more dominant role in the temporal variability of spring chemistry. Consequently, any characterization of karst aquifers using spring-water chemistry requires understanding the variety of sources of waters and their chemical compositions.

Acknowledgements

We acknowledge the staff at O'Leno State Park for their cooperation during this study, Mike Poucher for the line map of the conduits, and the many field assistants who helped collect samples. We thank two anonymous reviewers for their helpful remarks on an early draft of the paper. The work was supported by the Florida Department of Environmental Protection Grant Numbers S0060, S0141 and S0181, and NSF Grant Number EAR-510054.

References

- Bredehoeft, J.D., Papadopoulos, I.S., 1965. Rates of vertical groundwater movement estimated from the earth's thermal profile. *Water Resources Research* 1 (2), 325–328.
- Budd, D.A., Vacher, H.L., 2004. Matrix permeability of the confined Floridan Aquifer, Florida, USA. *Hydrogeology Journal* 12 (5), 531–549.
- Bush, P.W., Johnston, R.H., 1988. Ground-water hydraulics, regional flow, and ground-water development of the Floridan Aquifer system in Florida and in parts of Georgia, South Carolina and Alabama. US Geological Survey Professional Paper 1403-C, 80 p.
- Chelette, A.R., Pratt, T.R., Katz, B.G., 2003. Nitrate loading as an indicator of nonpoint source pollution in the lower St Marks–Wakulla Rivers watershed. Northwest Florida Water Management District Water Resources Special Report 02-1, 138 p.
- Chen, K., Jiao, J.J., Huang, J., Huang, R., 2007. Multivariate statistical evaluation of trace elements in groundwater in a coastal area in Shenzhen, China. *Environmental Pollution* 147 (3), 771–780.
- Crandall, C.A., Katz, B.G., Hirten, J.J., 1999. Hydrochemical evidence for mixing of river water and groundwater during high-flow conditions, lower Suwannee River basin, Florida, USA. *Hydrogeology Journal* 7, 454–467.
- Deming, D., 2002. Introduction to Hydrogeology. McGraw-Hill, New York. 468 p.
- Dingman, S.L., 2002. Physical Hydrology. Prentice Hall, Upper Saddle River, New Jersey. 646 p.
- Dreiss, S.J., 1989. Regional scale transport in a karst aquifer: 1. Component separation of spring flow hydrographs. *Water Resources Research* 25, 117–125.
- Edwards, L.E., Weedman, S.D., Simmons, K.R., Scott, T.M., Brewster-Wingard, G.L., Ishman, S.E., Carlin, N.M., 1998. Lithostratigraphy, Petrography, Biostratigraphy, and Strontium–Isotope Stratigraphy of the Surficial Aquifer System of Western Collier County, Florida. US Geological Survey Open-File Report 98-205, 79 p.
- EPA, 1983. Methods for the Chemical Analysis of Water and Wastes. Office of Research and Development, US Environmental Protection Agency, Cincinnati, Ohio, 552 p.
- Florea, L.J., 2006. The Karst of West-Central Florida (Ph.D. Diss.). University of South Florida.
- Florea, L.J., Vacher, H.L., 2006. Springflow hydrographs: eogenetic vs telogenetic karst. *Ground Water* 44 (3), 352–361.
- Florea, L.J., Vacher, H.L., 2007. Eogenetic karst hydrology: insights from the 2004 hurricanes, peninsular Florida. *Ground Water* 45 (4), 439–446.
- Ford, D.C., Williams, P.W., 2007. Karst Hydrogeology and Geomorphology. Wiley, Chichester, United Kingdom. 562 p.
- Fournier, M., Massei, N., Bakalowicz, M., Dussart-Baptista, L., Rodet, J., Dupont, J.P., 2007. Using turbidity dynamics and geochemical variability as a tool for understanding the behavior and vulnerability of a karst aquifer. *Hydrogeology Journal* 15 (4), 689–704.
- Freeze, R.A., Cherry, J.A., 1979. Groundwater. Prentice Hall, Englewood Cliffs, New Jersey. 290 p.
- Groszok, M., Ceryak, R., Allison, D., Cooper, R., Weinberg, M., Macesich, M., Enright, M.M., Rupert, F., 1992. Carbonate units of the Intermediate Aquifer system in the Suwannee River Water Management District, Florida. Florida Geological Survey, 22.
- Halihan, T., Sharp Jr., J.M., Mace, R.E., 2000. Flow in the San Antonio segment of the Edwards aquifer: matrix, fractures, or conduits? In: Sasowsky, I.D., Wicks, C.M. (Eds.), Groundwater Flow and Contaminant Transport in Carbonate Aquifers. A. A. Balkema, Rotterdam, Netherlands, pp. 29–146.
- Hanshaw, B.B., Back, W., 1979. Major geochemical processes in the evolution of carbonate–aquifer systems. *Journal of Hydrology* 43 (1–4), 287–312.
- Hess, J.W., White, W.B., 1988. Storm response of the karstic carbonate aquifer of south central Kentucky. *Journal of Hydrology* 99, 235–252.
- Hisert, R.A., 1994. A Multiple Tracer Approach to Determine the Ground and Surface Water Relationships in the Western Santa Fe River, Columbia County, Florida (Ph.D. Diss.). University of Florida, 211 p.
- Hughes, J.D., Vacher, H.L., Sanford, W.E., 2007. Three-dimensional flow in the Florida platform: Theoretical analysis of Kohout convection at its type locality. *Geology* 35 (7), 663–666.
- Hunn, J.D., Slack, L.J., 1983. Water resources of the Santa Fe River Basin, Florida, US Geological Survey Water-Resources Investigations Report 83-4075, 105 p.
- Jolliffe, I.T., 2002. Principle Component Analysis. Springer, New York. 487 p.
- Jones, I.C., Vacher, H.L., Budd, D.A., 1993. Transport of calcium, magnesium and SO₄ in the Floridan aquifer, west-central Florida: implications to cementation rates. *Journal of Hydrology* 143, 455–480.
- Junge, C.E., Werby, R.T., 1958. The concentration of chloride, sodium, potassium, calcium, and sulfate in rain water of over the United States. *Journal of the Atmospheric Sciences* 15 (5), 417–425.
- Katz, B.G., 2004. Sources of nitrate contamination and age of water in large karstic springs of Florida. *Environmental Geology* 46, 689–706.
- Katz, B.G., Böhlke, J.K., Hornsby, H.D., 2001. Timescales for nitrate contamination of spring waters, northern Florida, USA. *Chemical Geology* 179, 167–186.
- Katz, B.G., Chelette, A.R., Pratt, T.R., 2004. Use of chemical and isotopic tracers to assess sources of nitrate and age of ground water, Woodville Karst Plain, USA. *Journal of Hydrology* 289, 36–61.
- Katz, B.G., Catches, J.S., Bullen, T.D., Michel, R.L., 1998. Changes in the isotopic and chemical composition of ground water resulting from a recharge pulse from a sinking stream. *Journal of Hydrology* 211 (1–4), 178–207.
- Kautz, R., Stys, B., Kawula, R., 2007. Florida vegetation 2003 and land use change between 1985–1989 and 2003. *Florida Scientist* 70 (1), 12–23.
- Knochemus, L.A., Robinson, J.L., 1996. Descriptions of anisotropy and heterogeneity and their effect on ground-water flow and areas of contribution to public supply wells in a karst carbonate aquifer system. US Geological Survey Water-Supply Paper 2475, 47 p.
- Kohout, F.A., Henry, H.R., Banks, J.E., 1977. Hydrogeology related to geothermal conditions of the Floridan Plateau. In: Smith, K.L., Griffen, G.M. (Eds.), The Geothermal Nature of the Floridan Plateau, vol. 21. Florida Department of Natural Resources, Bureau of Geology Special Publication, pp. 1–41.
- Krothe, N.C., Libra, R.D., 1983. Sulfur isotopes and hydrochemical variations of spring waters of southern Indiana, USA. *Journal of Hydrology* 81, 267–283.
- Laaksoharju, M., Tullborg, E.-L., Wikberg, P., Wallin, B., Smellie, J., 1999. Hydrogeochemical conditions and evolution at the Äspö HRL, Sweden. *Applied Geochemistry* 14 (7), 835–859.
- Lakey, B., Krothe, N.C., 1996. Stable isotopic variation of storm discharge from a perennial karst spring, Indiana. *Water Resources Research* 32, 721–731.
- Lawrence, F.W., Upchurch, S.B., 1982. Identification of recharge areas using geochemical factor analysis. *Ground Water* 20, 680–687.
- Lazareva, O., Pichler, T., 2007. Naturally occurring arsenic in the Miocene Hawthorn Group, southwestern Florida: potential implication for phosphate mining. *Applied Geochemistry* 22 (5), 953–973.
- Lee, E.S., Krothe, N.C., 2001. A four-component mixing model for water in a karst terrain in south-central Indiana, USA. Using solute concentration and stable isotopes as tracers. *Chemical Geology* 179 (1–4), 129–143.
- Loper, D.E., Werner, C.L., Chicksen, E., Davies, G., Kincaid, T., 2005. Coastal Carbonate Aquifer Sensitivity to Tides. Eos, Transactions, American Geophysical Union 86 (39).
- Lu, N., Ge, S., 1996. Effect of horizontal heat and fluid flow on the vertical temperature distribution in a semi-confining layer. *Water Resources Research* 32 (5), 1449–1453.
- Martin, J.B., Dean, R.W., 1999. Temperature as a natural tracer of short residence times for ground water in karst aquifers. In: Palmer, A.N., Palmer, M.V., Sasowsky, I.D. (Eds.), Karst Modeling. Karst Waters Institute Special Publication 5, pp. 236–242.
- Martin, J.B., Dean, R.W., 2001. Exchange of water between conduits and matrix in the Floridan Aquifer. *Chemical Geology* 179, 145–165.
- Martin, J.B., Gordon, S.L., 2000. Surface and ground water mixing, flow paths, and temporal variations in chemical compositions of karst springs. In: Sasowsky, I.D., Wicks, C.M. (Eds.), Groundwater Flow and Contaminant Transport in Carbonate Aquifers. A.A. Balkema, Rotterdam, Netherlands, pp. 5–92.
- Martin, J.M., Sreaton, E.J., Martin, J.B., 2006. Monitoring well responses to karst conduit head fluctuations: Implications for fluid exchange and matrix transmissivity in the Floridan aquifer. In: Wicks, C.M., Harmon, R.S. (Eds.), Perspectives on Karst Geomorphology, Hydrology, and Geochemistry: A Tribute Volume to Derek C. Ford and William B. White. Geological Society of America, Boulder, Colorado, pp. 09–217.
- McConnell, J., Hacke, C.M., 1993. Hydrogeology, water quality, and water resources development potential of the Upper Floridan aquifer in the Valdosta area, south-central Georgia. US Geological Survey Water-Research Investigations Report 93-4044, 44 p.
- Melloul, A., Collin, M., 1992. The 'principal components' statistical method as a complementary approach to geochemical methods in water quality factor identification; application to the Coastal Plain aquifer of Israel. *Journal of Hydrology* 140 (1–4), 49–73.

- Miller, J.A., 1986. Hydrogeologic framework of the Floridan aquifer system in Florida and parts of Georgia, Alabama, and South Carolina. US Geological Survey Professional Paper 1403-B, 91 p.
- Moore, P.J., Martin, J.B., 2005. Exchange of water between conduit and matrix porosity in eogenetic karst? Evidence from a quantitative dye trace. Geological Society of America Abstracts with Programs 37 (7), 435.
- Olofsson, B., Jernberg, H., Rosenqvist, A., 2006. Tracing leachates at waste sites using geophysical and geochemical modelling. Environmental Geology 49 (5), 720–732.
- Phelps, G.G., 2001. Geochemistry and Origins of Mineralized Waters in the Floridan Aquifer System, Northeastern Florida. US Geological Survey Water-Resources Investigations Report 01-4112, 64 p.
- Plummer, L.N., 1977. Defining reactions and mass transfer in part of the Floridan Aquifer. Water Resources Research 13, 801–812.
- Plummer, L.N., Back, W., 1980. The mass balance approach; application to interpreting the chemical evolution of hydrologic systems. American Journal of Science 280 (2), 130–142.
- Plummer, L.N., Busenberg, E., McConnell, J.B., Drenkard, S., Schlosser, P., Michel, R.L., 1998. Flow of river water into a Karstic limestone aquifer: 1. Tracing the young fraction in groundwater mixtures in the Upper Floridan Aquifer near Valdosta, Georgia. Applied Geochemistry 13 (8), 995–1015.
- Poucher, M., 2007. Old Bellamy Cave. <http://www.cavesurvey.com/ob_cave.htm> (accessed on 11/20/2008).
- Puri, H.S., and Vernon, R.O., 1964. Summary of the Geology of Florida and a Guidebook to the Classic Exposures. Florida Geological Survey Special Publication 5, 312 p.
- Quinlan, J.F., Davies, G.J., Jones, S.W., Huntoon, P.W., 1996. The applicability of numerical models to adequately characterize ground-water flow in karstic and other triple-porosity aquifers. In: Ritchey, J.D., Rumbaugh, J.O. (Eds.), Subsurface Fluid-Flow (Ground-Water and Vadose Zone) Modeling. American Society for Testing and Materials, West Conshohocken, Pennsylvania, pp. 114–133.
- Reel, D.A., Griffin, G.M., 1971. Potentially petroliferous trends in Florida as defined by geothermal gradients. Transactions of Gulf Coast Association of Geological Societies 21, 31–36.
- Ritorto, M., 2007. Impacts of diffuse recharge on transmissivity and water budget calculations in the unconfined karst aquifer of the Santa Fe River basin (Ms. Thesis). University of Florida, 145 p.
- Ritorto, M., Screamon, E.J., Martin, J.B., Moore, P.J., 2009. Magnitudes and chemical effects of diffuse and focused recharge in an eogenetic Karst aquifer: an example from the unconfined Floridan aquifer. Hydrogeology Journal 23. doi:10.1007/s10040-009-0460-0.
- Rose, S., 1989. The heavy-metal adsorption characteristics of Hawthorne Formation (Florida, USA) sediments. Chemical Geology 74 (3–4), 365–370.
- Scanlon, B.R., 1989. Physical controls on hydrochemical variability in the inner bluegrass karst region of central Kentucky. Ground Water 27 (5), 639–646.
- Scanlon, B.R., Thrailkill, J., 1987. Chemical similarities among physically distinct spring types in a karst terrain. Journal of Hydrology 89 (3–4), 259–279.
- Scott, T.M., 1988. The lithostratigraphy of the Hawthorn Group (Miocene of Florida). Florida Geological Survey Bulletin 59, 147.
- Screamon, E., Martin, J.B., Ginn, B., Smith, L., 2004. Conduit properties and karstification in the Santa Fe river sink-rise system of the Floridan aquifer. Ground Water 42, 338–346.
- Shuster, E.T., White, W.B., 1971. Seasonal fluctuations in the chemistry of limestone springs: a possible means for characterizing carbonate aquifers. Journal of Hydrology 14, 93–128.
- Sklash, M.G., Farvolden, R.N., 1979. The role of groundwater in storm runoff. Journal of Hydrology 43, 45–65.
- Smart, P.L., Hobbs, S.L., 1986. Characterisation of Carbonate Aquifers: A Conceptual Base. In: Proceedings of the Environmental Problems in Karst Terranes and Their Solutions Conference, Bowling Green, Kentucky. National Well Water Association, Dublin, Ohio, pp. 1–14.
- Smith, D.L., Fuller, W.R., 1977. Terrestrial heat flow values in Florida and the effects of the aquifer system. In: Smith, K.L., Griffen, G.M. (Eds.), The Geothermal Nature of the Floridan Plateau, vol. 21. Florida Department of Natural Resources, Bureau of Geology Special Publication, pp. 91–130.
- Smith, D.L., Lord, K.M., 1997. Tectonic evolution and geophysics of the Florida basement. In: Randazzo, A.F., Jones, D.S. (Eds.), The Geology of Florida. University Press of Florida Gainesville, Florida, pp. 3–26.
- Sprinkle, C.L., 1989. Geochemistry of the Floridan Aquifer System in Florida and in Parts of Georgia, South Carolina, and Alabama. US Geological Survey Professional Paper 1403-I, 105 p.
- Sprouse, B.E., 2004. Chemical and Isotopic Evidence for Exchange of Water Between Conduit and Matrix in a Karst Aquifer: An Example From the Santa Fe River Sink/Rise System (Ms. Thesis). University of Florida, 84 p.
- Stetzenbach, K.J., Farnham, I.M., Hodge, V.F., Johannesson, K.H., 1999. Using multivariate statistical analysis of groundwater major cation and trace element concentrations to evaluate groundwater flow in a regional aquifer. Hydrological Processes 13 (17), 2655–2673.
- Stetzenbach, K.J., Hodge, V.F., Guo, C., Farnham, I.M., Johannesson, K.H., 2001. Geochemical and statistical evidence of deep carbonate groundwater within overlying volcanic rock aquifers/aquifers of southern Nevada, USA. Journal of Hydrology 243 (3–4), 254–271.
- Ternan, J.L., 1972. Comments on the use of a calcium hardness variability index in the study of carbonate aquifers, with reference to the central Pennines, England. Journal of Hydrology 129, 87–108.
- Toran, L., Herman, E.K., White, W.B., 2007. Comparison of flowpaths to a well and spring in a karst aquifer. Ground Water 45 (3), 281–287.
- Toth, D., Katz, B., 2006. Mixing of shallow and deep groundwater as indicated by the chemistry and age of karstic springs. Hydrogeology Journal 14 (6), 1060–1080.
- Vacher, H.L., Mylroie, J.E., 2002. Eogenetic karst from the perspective of an equivalent porous medium. Carbonates and Evaporates 17 (2), 182–196.
- Vesper, D.J., White, W.B., 2004. Storm pulse chemographs of saturation index and carbon dioxide pressure: implications for shifting recharge sources during storm events in the karst aquifer at Fort Campbell, Kentucky/Tennessee, USA. Hydrogeology Journal 12 (2), 135–143.
- Wicks, C.M., Herman, J.S., 1994. The effect of a confining unit on the geochemical evolution of ground water in the Upper Floridan aquifer system. Journal of Hydrology 153, 139–155.
- White, W.B., 1988. Geomorphology and Hydrology of Karst Terrains. Oxford University Press, New York, 464 p.
- White, W.B., 1999. Conceptual models for karstic aquifers. In: Palmer, A.N., Palmer, M.V., Sasowsky, I.D. (Eds.), Karst Modeling, vol. 5. Karst Waters Institute Special Publication, pp. 11–16.
- Wold, S., Esbensen, K., Geladi, P., 1987. Principal component analysis. Chemometrics and Intelligent Laboratory Systems 2 (1–3), 37–52.
- Worthington, S.R.H., 1994. Flow velocities in unconfined carbonate aquifers. Cave and Karst Science 21, 21–22.
- Worthington, S.R.H., Ford, D.C., Cavies, G.J., 2000. Matrix, fracture and channel components of storage and flow in a Paleozoic limestone aquifer. In: Sasowsky, I.D., Wicks, C.M. (Eds.), Groundwater Flow and Contaminant Transport in Carbonate Aquifers. A.A. Balkema, Rotterdam, Netherlands, pp. 13–128.